UDC 544.6.018.42-16; 544.643.076.2

DOI: 10.15372/CSD2020199

Transport Properties of $Li_4Ti_5O_{12}/Li_2TiO_3$ Composites

A. V. KOZLOVA[1,2], N. F. UVAROV[1,2]

[1]*Institute of Solid State Chemistry and Mechanochemistry, Siberian Branch, Russian Academy of Sciences, Novosibirsk, Russia*

E-mail: koza0707@yandex.ru

[2]*Novosibirsk State Technical University, Novosibirsk, Russia*

Abstract

Ceramic samples of lithium titanate spinel $Li_4Ti_5O_{12}$ and $Li_4Ti_5O_{12}/Li_2TiO_3$ composites with different content of Li_2TiO_3 as an additional phase were obtained by means of solid-phase synthesis. The phase composition and transport properties of the obtained samples are investigated. By means of impedance spectroscopy within the frequency range 20 Hz–1 MHz, three contributions into total resistance of the samples were discovered. Assumptions concerning the reasons for higher direct-current conductivity of $Li_4Ti_5O_{12}/Li_2TiO_3$ composites at room temperature than that of lithium titanate spinel $Li_4Ti_5O_{12}$ are made.

Keywords: lithium titanate spinel, $Li_4Ti_5O_{12}/Li_2TiO_3$ composites, ionic conductivity, grain boundary resistance

INTRODUCTION

Lithium ion batteries (LIB) are widely used as chemical energy sources for mobile phones, laptops, electric vehicles, etc. The most widespread anode material for LIB is graphite. One of the shortcomings of graphite anodes is a sharp decrease in charge capacity during cycling [1]. The reason for this behaviour is in substantial deformations in the layered structure of graphite while intercalation/deintercalation of lithium ions occur during charging/discharging processes. As a result, the destruction of crystallites takes place, which causes worsening of contacts between the grains and current collector, thus the resistance of the electrode increases. In parallel, the destruction and renewal of the solid electrolyte layer formed at the electrode during charging take place, which leads to the contamination of the electrolyte with the products of layer destruction. Gradually, the graphite layer becomes electrochemically passive, and instead of intercalaction, direct deposition of metal lithium may occur on the anode, in particular in the form of lithium dendrites [2], which has a negative effect on the reliability and safety of LIB.

Lithium titanate with spinel structure $Li_4Ti_5O_{12}$ (LTO) is considered as an alternative anode material. Unlike for graphite anode, this material does not undergo noticeable structural changes during charging/discharging [3] and does not form any solid electrolyte layer on grain surface, because it has a flat plateau with the high potential at about 1.5 V (in comparison with Li/Li^+) [4]. A small change in volume is connected with the fact that the crystal structures and unit cell parameters of LTO spinel and lithium-containing phase with the structure of rock salt type $Li_7Ti_5O_{12}$ are very close to each other [5]. A disadvantage of LTO is its low electronic (10^{-13} S/cm) and ionic (less than 10^{-9} S/cm) conductivity, which explains insufficient efficiency of recharging processes at high charging – recharging rates. In spite of this fact, LTO remains one of the most promising anode materials for rechargeable batteries because this material possesses high

reliability and excellent cycling capacity. The proposals for the improvement of LTO characteristics include several versions of doping with different ions [6–9], a decrease in particle size [10], modification of the surface using conductive coatings [11]. It has been demonstrated recently that LTO/Li_2TiO_3 composites possess good cycling capacity at the high charging/discharging rate 10C, and the addition of electrochemically inactive Li_2TiO_3 provides the stability of microstructure of the active material LTO [12]. In [13], the effect of Li_2TiO_3 addition on the electrochemical properties of LTO was studied in the composites obtained in the form of nanofibres by means of electrospinning. It was discovered that the charge capacity of LTO/Li_2TiO_3 nanocomposites exceeds the corresponding values for LTO. The reasons for this effect remain unclear.

In the present work, we describe the studies of the ion conductivity of LTO and the composites LTO/Li_2TiO_3 carried out by means of impedance spectroscopy for the purpose of revealing the reasons of the influence of Li_2TiO_3 addition on the electrochemical properties of LTO.

EXPERIMENTAL

LTO and LTO/Li_2TiO_3 composites were synthesized using the solid-phase method from initial reagents: TiO_2 and Li_2CO_3 (Kh. Ch. reagent grade). To obtain pure LTO, we used initial components with the molar ratio Li/Ti = 4 : 5 according to the stoichiometric composition. To prepare the composites corresponding to the calculated compositions $0.8LTO/0.2Li_2TiO_3$ (LTC20) and $0.7LTO/0.3Li_2TiO_3$ (LTC30), the molar ratio Li/Ti was 4.8 : 5 and 5.2 : 5, respectively. Initial mixtures were subjected to mechanical treatment in an AGO-2 ball mill for 5 min with the rotation frequency of 400 r.p.m., then the samples were pressed in pellets. The synthesis was carried out at a temperature of 900 °C for 5 h.

The crystal structure of the obtained samples was analyzed by means of X-ray phase analysis with the help of a Bruker Advance D8 diffractometer (Germany) with CuK_α-radiation. Phases were identified using the ICDD-PDF2 database.

Measurements of the conductivity of LTO and composites were carried out using a two-electrode scheme with the electrodes deposited from the silver paste. Measurements were carried out by means of impedance spectrometry within the low-temperature region (25–250 °C) in vacuum and at high temperature (200–600 °C) in the air with the help of a HP-4184A Precision LCR Meter (USA) within the frequency range of variable field from 20 Hz to 1 MHz. The temperature was changed stepwise under the control with the help of a Termodat temperature controller. Conductivity values were calculated from an analysis of the hodographs of complex impedance $Z'' = f(Z')$.

RESULTS AND DISCUSSION

Diffraction patterns of the obtained LTO and LTC30 composite samples are shown in Fig. 1. The diffraction pattern of the composite (see Fig. 1, *b*) contains overlapping diffraction peaks of LTO and Li_2TiO_3. The lattice parameters of LTO and Li_2TiO_3 phases in the composite were refined using the Rietveld method. These values turned out to be close to those reported in the literature. Diffraction data were used also to determine the phase composition of the composites, which corresponded to the values calculated from the amounts of initial reagents with the accuracy of ±10 %.

Temperature dependencies of the conductivity (σ) of LTO and LTC20, LTC30 composites are presented in Arrhenius coordinates in Fig. 2. Conductivity σ was calculated from sample resistance (R) with the help of equation

$$\sigma = (1/R)\,(L/S)$$

where S is electrode area, L is pellet thickness. Sample resistance R was determined by fitting the theoretical parameters of standard equivalent schemes to the experimental values of the real (Z′) and imaginary (Z″) components of complex impedance (Z*). The values of σ are well reproduced in heating/cooling cycles. Therefore, conductance occurs not due to surface conductivity or metastable defects but it is an equilibrium characteristic of the substance.

Analysis of the spectra of complex impedance, the frequency and temperature dependencies of conductivity showed that the experimentally measured impedance of LTO is described by the equivalent circuit consisting of three serially connected (R/CPE)-elements, where CPE is a constant phase element (see Fig. 2). Each element of the circuit corresponds to a separate stage of ion transfer in the material.

The first element of the equivalent circuit describes the fastest stage, which is characterized

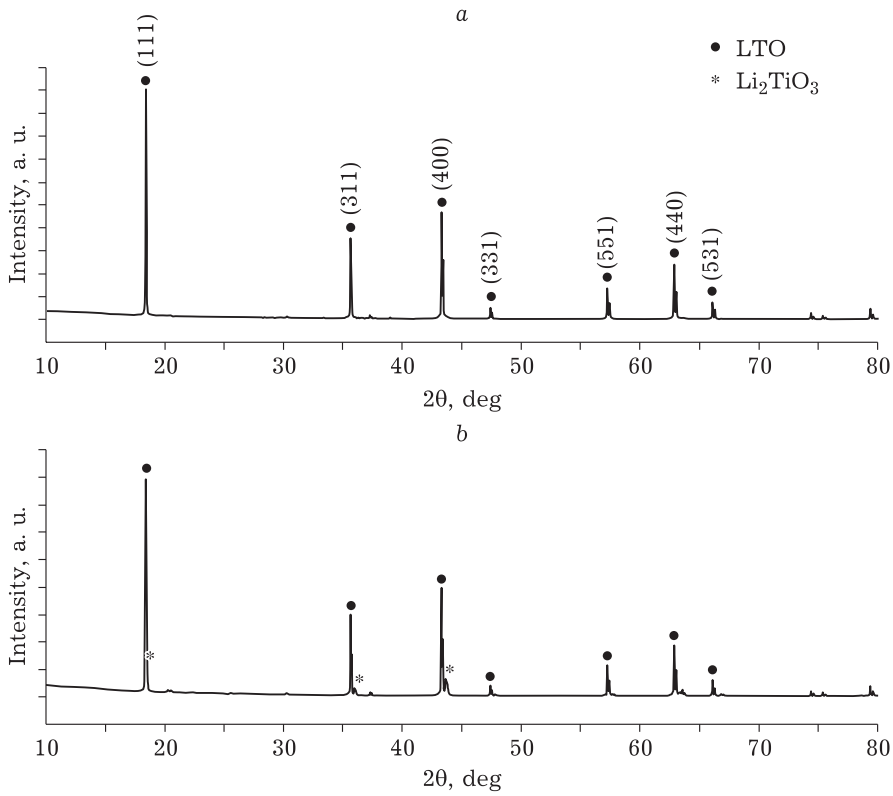

Fig. 1. Diffraction patterns of LTO (*a*) and LTC30 composite (*b*).

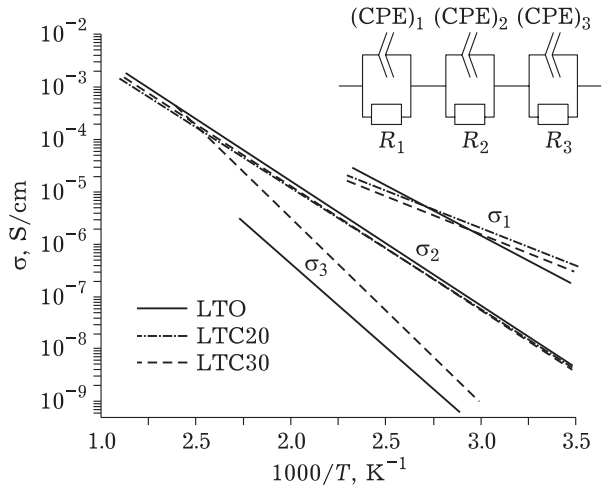

Fig. 2. Comparison of the temperature dependencies of the conductivities of LTO and LTC20, LTC30 composites. The equivalent electric circuit used to interpret the data obtained by means of impedance spectroscopy is shown in the insert in the upper part. The values of σ_1, σ_2 and σ_3 correspond to the elements with resistance R_1, R_2 and R_3 of the equivalent circuit.

by the highest conductivity σ_1 with the lowest activation energy $E_1 = 0.31$ eV. This stage is likely to be due to local jumps of lithium cations in LTO lattice. It was established on the basis of the results of ab initio modeling by means of molecular dynamics that the distribution of energy barriers for the conductivity of lithium ions is extremely complicated. As a consequence of random distribution of lithium and titanium atoms, the major positions of lithium in the lattice are nonequivalent. Calculation results show that the lowest energy barrier corresponding to local displacements of lithium cations is about 0.30 eV [14]. The possibility of migration for lithium ions with low activation energy was predicted by theoretical estimations described in [15]. These data are confirmed by the presence of the contribution from high-frequency conductivity with low activation energy in the samples under study. A similar contribution provided by the presence of LTO is observed also in LTC20 and LTC30 composites.

The second element of the equivalent circuit describes ion transfer through the volume of the material and is characterized by volume conductance σ_2 with activation energy $E_2 = 0.60$ eV. This activation energy is in agreement with calculation data described in [14]. The value of LTO conductivity at room temperature as determined by us ($2.5 \cdot 10^{-9}$ S/cm) gets within the

range of values reported in the literature: from $8 \cdot 10^{-10}$ [16] to $7.6 \cdot 10^{-8}$ S/cm [17]. Low conductivity values may be explained by the absence of vacancies in 8*a* positions and interstitial lithium ions in 16*c* positions of the spinel structure.

The third element of the equivalent circuit describes the transfer of ions through intergrain boundaries and is characterized by the effective conductivity σ_3 with activation energy E_3 = 0.76 eV. This process is limited by the contribution from grain boundaries into the total impedance of the sample.

Sample conductivity measured at the direct current, $\sigma_{dc} = 1/(1/\sigma_1 + 1/\sigma_2 + 1/\sigma_3)$, is limited at low temperatures by σ_3 value. This value, determined by the resistance of grain boundaries, depends on the size of particles in the samples, pellet density and the presence of impurities adsorbed on grain boundaries. The addition of a small amount of Li_2TiO_3 into LTO leads to a decrease in the resistance of grain boundaries and an increase in σ_3. In spite of the difference in the symmetry of crystal structures, LTO and Li_2TiO_3 possess similar chemical and physical characteristics, their densities at room temperature differ by 1.5 %. Therefore, it may be expected that adhesion between LTO and $Li_2TiO_3$is strong, and a good interfacial contact is formed between the components during sintering of their mixture. Additional point defects may arise at the LTO/Li_2TiO_3 interface due to the surface interaction between the phases, accompanied by the transfer of cations from one phase into another. Similar processes are characteristic of composite solid electrolytes [18]. The change of morphology with the transition from LTO to composites is shown schematically in Fig. 3. As a result, the concentration of charge carriers near the interface increases, which leads to a decrease in the resistance of the grain boundary (an increase in σ_3) for LTC20 sample to the values comparable with the volume conductivity of LTO. Because of this, there is no contribution from the second element of the equivalent circuit into total impedance of this composite (see Fig. 2). With an increase in the concentration of Li_2TiO_3 , the contacts between LTO particles get broken as a consequence of an increase in the number of particles of the dielectric phase Li_2TiO_3 , which leads to an increase in the resistance of grain boundaries. As a result, σ_3 becomes substantially lower than the volume conductivity of LTO.

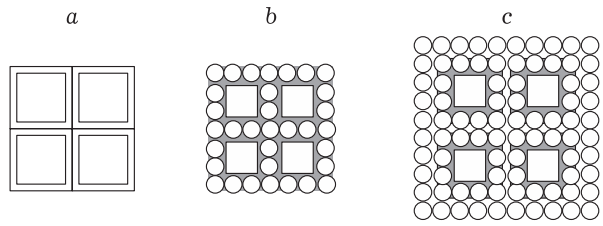

Fig. 3. Schematic representation of the change of morphology when going from LTO (*a*) to composites LTC20 (*b*) and LTC30 (*c*). Large squares are LTO particles with blocking layers near grain boundaries; spheres are Li_2TiO_3 particles; dark regions are conducting regions in the vicinity of LTO/Li_2TiO_3 interfaces.

Because of relatively high conductivity of composites with respect to LTO, the electrodes made of LTO/Li_2TiO_3 may operate at higher charging and discharging modes. In addition, they possess higher charging capacity due to the effect of the boundaries between the phases, which provides the appearance of new positions in Li_2TiO_3 structure in which lithium cations may be arranged [9].

CONCLUSION

The conductivity of ceramic LTO and composite LTO/Li_2TiO_3 samples containing different amounts of Li_2TiO_3 is investigated. Using impedance spectrometry, three contributions into the total resistance of samples were distinguished. These contributions correspond to fast local motions of lithium cations in the structure (σ_1), volume conductivity (σ_2) of the sample, and the contribution determined by the resistance of grain boundaries in the ceramics (σ_3). Conductivity values measured at the direct current at room temperature are higher in the composites than in LTO, which is explained by a lower resistance of grain boundaries due to the effect of LTO/Li_2TiO_3 interfaces in the composites.

REFERENCES

1 Ribiere P., Grugeon S., Morcrette M., Boyanov S., Laruellea S., Marlair G., Investigation on the fire-induced hazards of Li-ion battery cells by fire calorimetry, *Energy Environ. Sci.*, 2012, Vol. 5, P. 5271–5280.

2 Xiang H. F., Zhang X., Jin Q. Y., Zhang C. P., Chen C. H., Ge X. W., Effect of capacity match up in the $LiNi_{0.5}Mn_{1.5}O_4$/$Li_4Ti_5O_{12}$ cells, *J. Power Sources*, 2008, Vol. 183, P. 355–360.

3 Ohzuku T., Ueda A., Yamamoto N., Zero-strain insertion material of $Li[Li_{1/3}Ti_{5/3}]O_4$ for rechargeable lithium cells, *J. Electrochem. Soc.*, 1995, Vol. 142, P. 1431–1435.

4 Zhu G. N., Wang Y. G., Xia Y. Y., Ti-based compounds as anode materials for Li-ion batteries, *Energy Environ. Sci.*, 2012, No. 5, P. 6652–6667.
5 Scharner S., Weppner W., Schmid-Beurmann P., Evidence of two-phase formation upon lithium insertion into the $Li_{1.33}Ti_{1.67}O_4$ spinel, *J. Electrochem. Soc.*, 1999, Vol. 146, No. 3, P. 857–861.
6 Ji S., Zhang J., Wang W., Huang Y., Feng Z., Zhang Z., Tang Z., Preparation and effects of Mg-doping on the electrochemical properties of spinel $Li_4Ti_5O_{12}$ as anode material for lithium ion battery, *Mater. Chem. Phys.*, 2010, Vol. 123, P. 510–515.
7 Lin C., Lai M. O., Lu L., Zhou H., Xin Y., Structure and high rate performance of Ni^{2+} doped $Li_4Ti_5O_{12}$ for lithium-ion battery, *J. Power Sources*, 2013, Vol. 244, P. 280–287.
8 Li X., Qu M., Yu Z., Structural and electrochemical performances of $Li_4Ti_5{-}xZr_xO_{12}$ as anode material for lithium-ion batteries, *J. Alloys Compd.*, 2009, Vol. 487, No. 13, P. L12–L17.
9 Yi T. F., Shu J., Zhu Y. R., Zhu X. D., Yue C. B., Zhou A. N., Zhu R. S., High-performance $Li_4Ti_5{-}xV_xO_{12}$ ($0 < x < 0.3$) as an anode material for secondary lithium-ion battery, *Electrochim. Acta*, 2009, Vol. 54, P. 7464–7470.
10 Zhu G. N., Liu H. J., Zhuang J. H., Wang C. X., Wang Y. G., Xia Y. Y., Carbon-coated nano-sized $Li_4Ti_5O_{12}$ nanoporous micro-sphere as anode material for high-rate lithium-ion batteries, *Energy Environ. Sci.*, 2011, No. 4, P. 4016–4022.
11 Tang Y., Huang F., Zhao W., Liu Z., Wan D., Synthesis of graphene-supported $Li_4Ti_5O_{12}$ nanosheets for high rate battery application, *J. Mater. Chem.*, 2012, No. 22, P. 11257–11260.
12 Wang Y., Zhou A., Dai X., Feng L., Li J., Solid-state synthesis of submicron-sized $Li_4Ti_5O_{12}/Li_2TiO_3$ composites with rich grain boundaries for lithium ion batteries, *J. Power Sources*, 2014, Vol. 266, P. 114–120.
13 Li S., Guo J., Ma Q., Yang Y., Dong X., Yang M., Yu W., Wang J., Liu G., Electrospun $Li_4Ti_5O_{12}/Li_2TiO_3$ composite nanofibers for enhanced high-rate lithium ion batteries, *J. Solid State Electrochem.*, 2017, Vol. 21, P. 2779–2790.
14 Weber V., Laino T., Curioni A., Eckl T., Engel C., Kasemchainan J., Salingue N., Computational study of lithium titanate as a possible cathode material for solid-state lithium-sulfur batteries, *J. Phys. Chem. C*, 2015, Vol. 119, P. 9681–9691.
15 Ziebarth B., Klinsmann M., Eckl T., Lithium diffusion in the spinel phase $Li_4Ti_5O_{12}$ and in the rocksalt phase $Li_7Ti_5O_{12}$ of lithium titanate from first principles, *Phys. Rev. B*, 2014, Vol. 89, P. 174301-1–174301-7.
16 Wolfenstine J., Allen J. L., Electrical conductivity and charge compensation in Ta doped $Li_4Ti_5O_{12}$, *J. Power Sources*, 2008, Vol. 180, P. 582–585.
17 Wang J., Yang Z., Li W., Zhong X., Gu L., Yu Y., Nitridation Br-doped $Li_4Ti_5O_{12}$ anode for high rate lithium ion batteries, *J. Power Sources*, 2014, Vol. 266, P. 323–331.
18 Uvarov N. F., Composite solid electrolytes: recent advances and design strategies, *J. Solid State Electrochem.*, 2011, Vol. 15, P. 367–389.